Int. J. Electrochem. Sci., 13 **(2018)** 5513 – 5521, doi: 10.20964/2018.06.78

International Journal of
ELECTROCHEMICAL
SCIENCE
www.electrochemsci.org

Effect of Ag-Te doped Glass Frits on Interface Reaction and the Electrical Properties of Silicon Solar Cells

Feng Xiang, Wei-Ping Gan

School of Material Science and Engineering, Central South University, Changsha 410083, China.
*E-mail: 28977845@qq.com

Received: 12 October 2017 / *Accepted:* 11 April 2018 / *Published:* 10 May 2018

In this study, a new Ag-Te doped glass frits were used to prepare silver pastes in order to improve the electrical properties of silicon solar cells. A set of silver pastes was formulated to investigate the effect of the doping proportion on the electrical properties of the silicon solar cells. The silver paste with 5wt% dopant increased the photovoltaic conversion efficiency of silicon solar cells by 0.199% compared to the increase achieved using the paste without the dopant. This effect could be attributed to the addition of dopant, which increased the size and number of Ag crystallites on the silicon wafer. The size and number of Ag crystallites were the major factors controlling the contact resistance between the silver electrode and the silicon wafer, and series resistance of solar cells. When the dopant proportion reached 10wt% or 15wt%, the p-n junction broke due to the oversized Ag crystallites embedded in the p-n junction. Thus, the leakage current was observed, and this current degraded the electrical properties of the silicon solar cells. Therefore, the proper proportion of Ag-Te doped glass frits was necessary to obtain the optimal the silicon solar cells.

Keywords: Ag-Te doped glass frits; Ag crystallites; electrical properties; solar cells

1. INTRODUCTION

In industrial silicon solar cells, screen-printed silver electrodes are typically used for the front side metallization. The silver paste most commonly used for the emitter contacts contains Ag powders, glass frits and an organic carrier. The Ag powders serve as the conducting phase and allow the electrons generated within the silicon to flow through the device. The glass frits etch the SiNx anti-reflection, dissolve a small amount of the Ag powders, react with the silicon and promote the precipitation of Ag crystallites on the silicon during the firing process. The organic carrier thoroughly disperses the solid powders and improves the quality of screen printing[1, 2].

As reported by previous works[3, 4], the industrial glass frits for the silver paste almost lead-tellurite glass frits, which has excellent electrical and mechanical properties. The metallic nanozinc and zinc oxide, which had been doped to lead-base glass frits, provide more uniform etching of the SiNx anti-reflection resulted in the lower contact resistance. With the optimization of the composition of glass frits, the melted glass could etch the SiNx anti-reflection completely by itself. The silver nanoparticles also had been prepared for the silver paste to improve the electrical properties of silicon solar cells. The silver nanoparticles could be a good dopant to obtain dense and compact thick film due to their excellent sintering behavior. However, the size, morphology and dispersion of the silver nanoparticles were difficult to control during the preparation process. Therefore, those materials could not be used for the industrial silver paste.

In previous studies[5-7], the melted glass dissolves a small amount of the Ag powders and promoted the precipitation of Ag crystallites on the silicon during the firing process. The size and number of Ag crystallites have a substantial impact on the transport current, the contact resistance between the silver electrode and the silicon wafer and the electrical properties of the solar cell. The Ag content in the melted glass, the constituents of the glass and the firing process determine the size and number of Ag crystallites. The firing process lasted only a few seconds; thus, the Ag powders do not completely melt. Therefore, the amount of Ag in the melted glass is limited. Theoretically, a higher Ag content in the melted glass can provide more Ag crystallites during firing. A higher number of Ag crystallites can decrease the contact resistance; thus, increasing the number of crystallites is required to synthesize proper lead-tellurite glass frits[8], which contain silver alloy powders with lower melting temperatures than the softening temperature of the glass frits. Then, the silver alloy powders and glass frits melt and react in the early stage of the firing process, which can increase the Ag content in the liquid glass. As the alloying component, tellurium has good electrical conductivity and it less toxic than Pb. Fig. 1 shows the phase diagram of the Ag-Te system[9]. The melting temperature of the Ag-Te alloy with 70.3wt% tellurium would be 353°C, which is much lower than the softening temperature of the glass frits (543°C)[8]. Herein, different amounts of Ag-Te powders have been doped to the glass frits to optimize the precipitation of Ag crystallites during the sintering of the frits and ultimately improve the photovoltaic properties of the silicon solar cells.

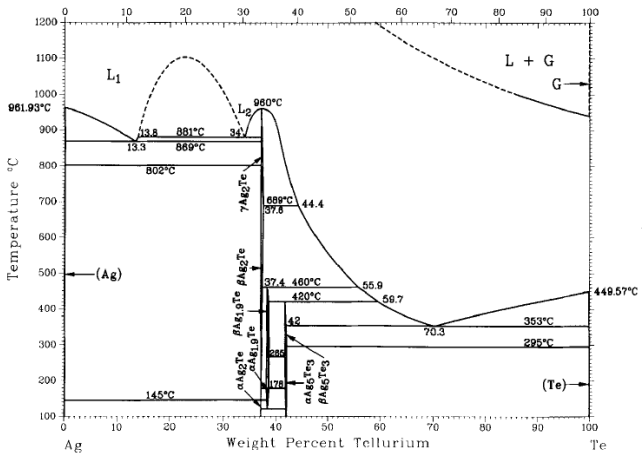

Figure 1. Phase diagram of the Ag-Te system

2. EXPERIMENTAL

Ag-Te powders have been prepared by melting and ball milling. Silver powder (S119033, Aladdin, 99.99% purity) and tellurium powder (T108767, Aladdin, 99.9% purity) were used to prepare the Ag-Te powders. The amounts of silver powder and tellurium powder used were 29.7wt% and 70.3wt%, respectively. They were weighed and mixed in an alumina crucible for 3 hours. The mixed powders were melted at 1000℃ for 1 hour in a furnace, and then the melted fluid was poured into deionized water. The alloy was pulverized under wet conditions by using a planetary mill to obtain the Ag-Te powder.

Paste A was prepared by mixing the glass frits powder (70wt%), Ag-Te powder (15wt%) and diethylene glycol monobutyl ether (15wt%) in an agate mortar for 30 minutes. To observe the Ag precipitation behavior of the doped glass frits, the Paste A was screen-printed on the silicon wafer with a SiNx layer. The screen-printed paste was heated at 800°C for 5 minutes in a muffle furnace.

Four different batches of pastes were prepared in study. The doped glass frits were prepared by mixing the glass frits and Ag-Te powders in a rotary mixer for 3 hours. The proportion of Ag-Te powders to the glass frits were 0%, 5%, 10% and 15%, respectively. Table 1 shows the batch compositions of the silver pastes. Spherical silver powders with a mean diameter of ~1.5μm, the organic carrier (a mixture of diethylene glycol monobutyl ether, terpineol, ethyl cellulose ethoce and thixotropic agent) and different proportion of doped glass frits were pre-mixed by using a high speed mixer for 1 hour, and grounded by 3 roll milling for 5 times to disperse the powders in the organic carrier completely.

Table 1. Compositions of the silver pastes with different proportion Ag-Te doped glass frits

Paste	Composition (wt%)		
	Doped Glass frits (proportion of the Ag-Te powder doped in the glass frits, wt%)	Ag powder	Organic carrier
AP1	3(0)	88	9
AP2	3(5)	88	9
AP3	3(10)	88	9
AP4	3(15)	88	9

The four different pastes were screen-printed on the front side of solar cells (78 mm×78 mm) that had been printed with Al pastes and Ag pastes on the back side. Then, the solar cells were co-fired in an IR belt-line furnace with a peak temperature of 800°C and a belt speed of 230 in/min.

The microstructure of the Ag-Te powders, the contact between the doped glass frits and the solar cells and the contact between the silver electrodes and the solar cells were examined using scanning electron microscopy (SEM, MIRA3, TESCAN) in conjunction with energy dispersive

spectroscopy (EDS). The leakage current of the solar cells was determined using an EL (electroluminescence) tester for cells (OPT-C100). The electrical performance of the studied solar cells was determined using a solar simulator and a testing system (DLSX-FXJ7, Beijing Delicacy Laser Optoelectronics Co. Ltd).

3. RESULTS AND DISCUSSION

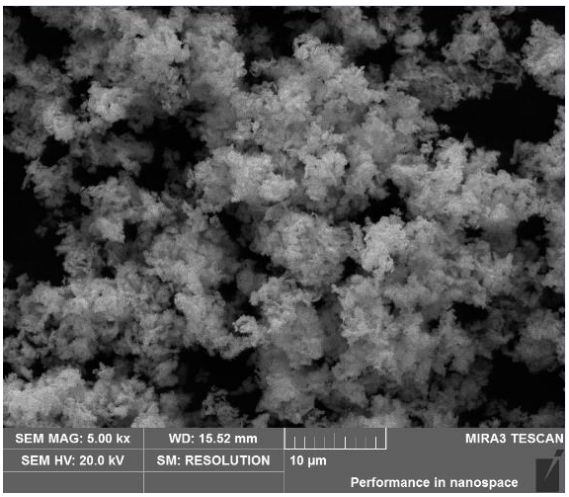

Figure 2. SEM image of the Ag-Te powders prepared by melting and ball milling

Ag-Te alloy powders were prepared by melting and ball milling. As shown in Fig. 1, the melting point of the as-prepared Ag-Te powders should be around 353°C. Fig. 2 shows the microstructure of the Ag-Te powders, and the surface of the powder showed flocculation.

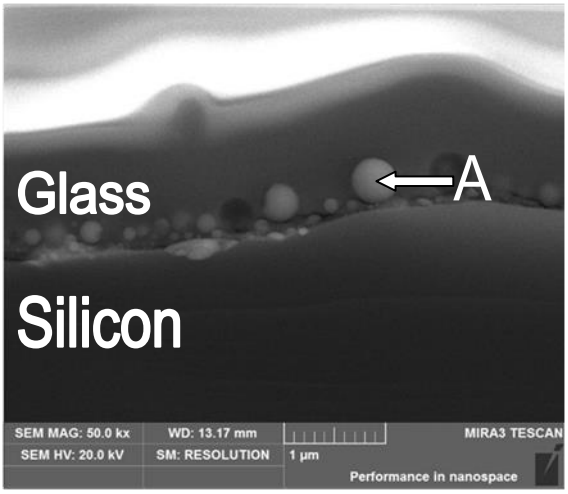

Figure 3. SEM image of the cross-sectional microstructures of Paste A fired on a silicon wafer

Fig. 3 shows the cross-sectional microstructure image of Paste A after firing on a silicon wafer at 800°C for 5 minutes. The doped glass frits completely melted and reacted with the silicon wafer

during the firing process. There are two mechanisms to explain the formation of Ag crystallites at the interface of an n+ emitter and silver bulk[10].

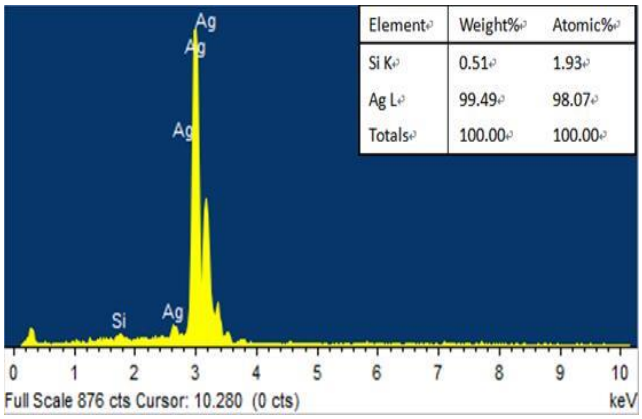

Figure 4. EDS spectrum analysis of point A in Figure3

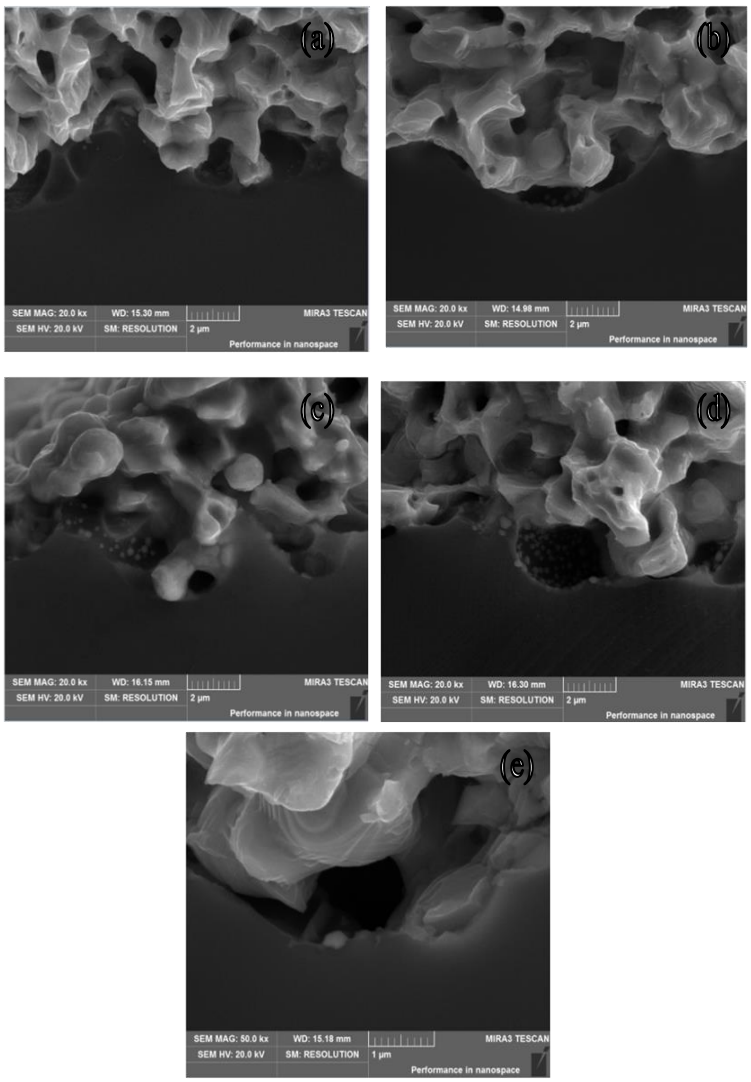

Figure 5. SEM image of the cross-sectional microstructures of silver electrodes prepared from the silver pastes with different proportion Ag-Te doped glass frits: (a) AP1, (b) AP2, (c) AP3, (d) and (e) AP4

The first mechanism involves the melted glass frits dissolved a small portion of the Ag particles during sintering. The melted glass can simultaneously etch and react with the SiNx layer to form liquid Pb. Moreover, the melted glass could rapidly react with Si to generate more liquid Pb. Then, the silver dissolved in the glass could react with the liquid Pb to form PbO and Ag crystallites. In the other mechanism, the Ag crystallites could be directly formed by a reaction between the silver dissolved in the melted glass and the silicon. The Ag crystallites can be seen in Fig. 4, which was obtained from point A in Fig. 3. A certain number of Ag crystallites are visible at the interface. The melted Ag-Te powder reacts with the glass frits. Then, the silver reacts with the liquid lead and silicon and forms Ag crystallites on the silicon surface. The tellurium from the Ag-Te powder remained in the glass after this process.

Fig. 5 shows the cross-sectional microstructures of the silver electrodes formed from AP1, AP2, AP3, AP4 and a silicon wafer. AP1 (Fig. 5a) was prepared without using doped glass frits. Fig. 5a shows a small number of tiny Ag crystallites randomly precipitated on the silicon surface. The limited solubility of Ag in the glass frits was the main reason for the precipitation of a small number of Ag crystallites. The size and number of Ag crystallites visible in Fig. 5b (AP2) were larger than those visible in Fig. 5a. During sintering, the glass frits softened, which dissolved the Ag powders, etched SiNx and reacted with silicon. The dopants also melted during sintering. The capillary attraction force due to the small spacing between the particles of silver powder caused the liquid phase to flow to the n^+ emitter[11], which allowed more silver to reach the region of the silicon where the liquid phase was located to form small Ag crystallites. Thus, the Ag crystallites tended to become coarser and ultimately form larger and more Ag crystallites. As the proportion of the doped powders increased, the silver concentration also increased. Therefore, the thermodynamic driving forces for the reaction was increased. The size and number of the Ag crystallites was expected to increase as the proportion of doped glass frits increased. This phenomenon can be observed in Fig. 5b, Fig. 5c and Fig. 5d. A large Ag crystallite embedded in the silicon wafer can be seen in Fig. 5e. In this study, larger and more Ag crystallites formed by using doped glass frits were expected to reduce the series resistance and improve the photovoltaic conversion efficiency of solar cells.

Fig. 6 shows the EL images of the solar cells with screen-printed AP1, AP2, AP3 and AP4. The EL data could be used to analyze the leakage current of the solar cells. The white spots in the EL images indicated the breakdown of the p-n junction, which causes leakage current and degrades the electrical properties of the cells. Interestingly, no white spots are present in Fig. 6a and Fig. 6b, indicating that AP1 and AP2 fired well during sintering. However, Fig. 6c and Fig. 6d show that the white spots appeared and increased when the dopant proportion was 10wt% and 15wt% (AP3 and AP4). As the proportion of doped glass frits increased, the melted doped glass more aggressively etched the silicon, which allowed the Ag to penetrate into the p-n junction. The Ag crystallites that grow at the n^+ emitter interface can cause p-n junction shunting, which in turn causes leakage current and has a negative influence on the electrical properties of the cells[12-14]. Oversized Ag crystallites embedded in the silicon wafer can be seen in Fig. 5e.

Fig. 7 shows the current-voltage(I-V) curves of the solar cells based on AP1,AP2,AP3 and AP4. The electrical parameters of the solar cells could be calculated from the I-V curves. Table 2 shows the electrical parameters of the solar cells manufactured by using AP1, AP2, AP3 and AP4.

Compared with those of the solar cells prepared using AP1, the solar cells screen-printed with AP2 shows superior electronic properties, which could be attributed to the doped glass frits. The Ag crystallites shown in Fig. 5b appear to be larger and of higher in quantity than that those visible in Fig. 5a. With increasing number and size of Ag crystallites, the silver electrode will likely be more directly connected to the silicon wafer. In addition, the current could easily pass through the ultra-thin glass region by tunneling since the larger Ag crystallites shortened the distance between the silver electrode and the Ag crystallites.

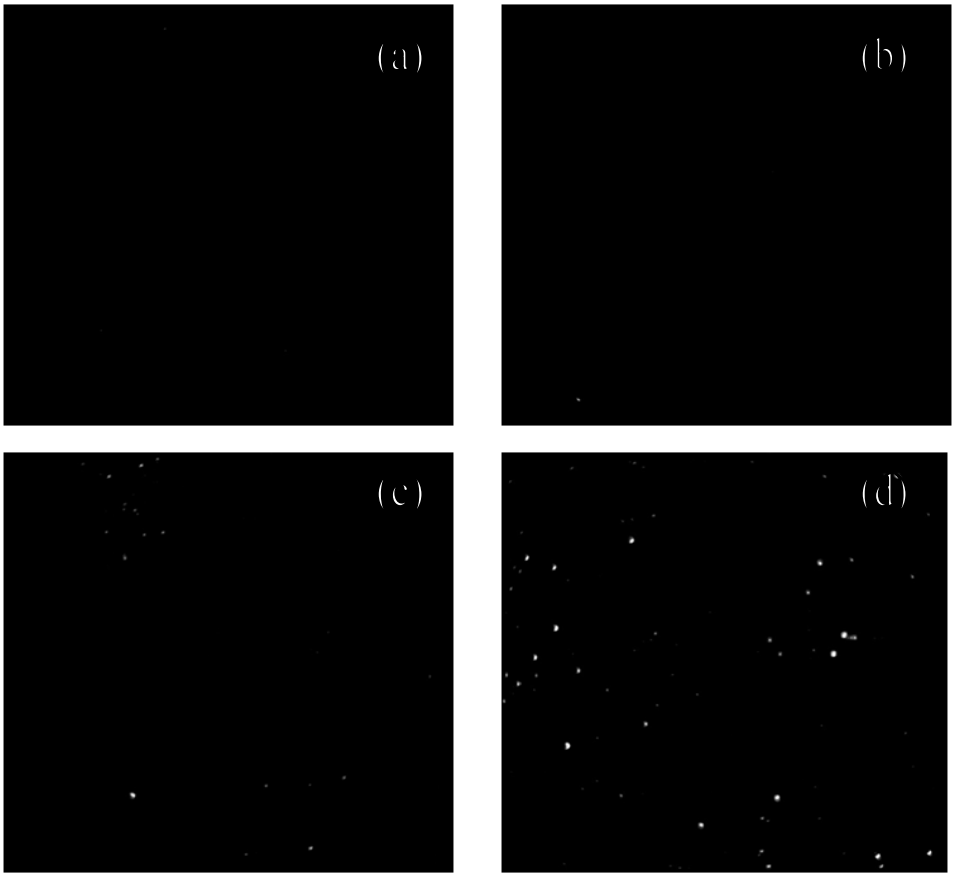

Figure 6. EL images of solar cells prepared from the silver pastes with different proportion Ag-Te doped glass frits: (a) AP1, (b) AP2, (c) AP3 and (d) AP4

Thus, these two effects decreased the contact resistance between the silver electrode and the silicon wafer, which is the main contributor to the series resistance of the solar cells[15-17].Thus, AP2 provided a lower series resistance (0.092Ω vs 0.096Ω), higher short circuit current (2.283 A vs 2.278 A), higher fill factor (0.774 vs 0.766) and higher photovoltaic conversion efficiency (18.393% vs 18.194%) than AP1. When the proportion of doped glass frits increased, the electrical properties of the solar cells gradually decreased, as seen in the properties of the cells prepared with AP3 and AP4. Integrating the EL images and the shunt resistance of the solar cells indicates that leakage current was generated at the p-n junction[18]. The silicon wafer was substantially etched by using a large proportion of doped glass frits; thus, the Ag crystallites nucleated in the etched pits. When the p-n

junction broke or became impure, the electron-hole pairs recombined and formed a leakage current. The leakage current caused the shunt resistance of AP3 (13.877Ω vs 39.843Ω) to be lower than that of AP1. The other electrical properties of AP3 appeared to be slightly worse than those of AP1 because the positive influence of the lower contact resistance and the negative influence of the leakage current cancel each other out. As the proportion of doped glass frits reached 15% in AP4, the balance between these two factors was destroyed. Hence, the shunt resistance rapidly decreased to 9.866Ω, and the photovoltaic conversion efficiency became lower (17.203%) than that seen with AP1.

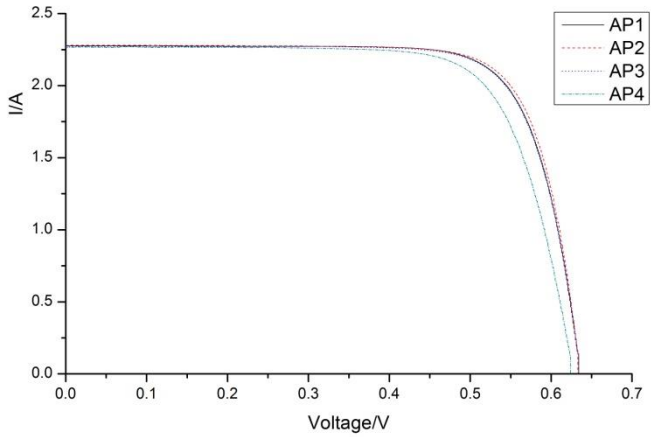

Figure 7. Current-Voltage(I-V) curves of the solar cells prepared from the silver pastes with different proportion Ag-Te doped glass frits: AP1,AP2,AP3 and AP4

Table 2. Electrical performances of the solar cells prepared from the silver pastes with different proportion Ag-Te doped glass frits: AP1, AP2, AP3 and AP4

Paste	Open circuit voltage (V_{oc})(V)	Shot circuit current (I_{sc})(A)	Series resistance (R_s)(Ω)	Shunt resistance (R_{sh})(Ω)	Fill factor (FF)	Photovoltaic conversion efficiency (E_{ff})(%)
AP1	0.634	2.278	0.096	39.843	0.766	18.194
AP2	0.634	2.283	0.092	100.028	0.774	18.393
AP3	0.634	2.276	0.100	13.877	0.765	18.154
AP4	0.624	2.269	0.107	9.866	0.739	17.203

4. CONCLUSION

In this study, it was found that the Ag-Te doped glass frits used in screen-printed Ag pastes can enhance Ag crystallite precipitation, reduce series resistance and enhance photovoltaic conversion efficiency of solar cells. A set of Ag pastes with different proportion of Ag-Te powders in the doped glass frits were formulated, screen-printed and fired. As the proportion of doped glass frits increased, the size and number of Ag crystallites increased, which reduced the contact resistance between the

silicon wafer and the silver electrode. This reduced contact resistance in turn reduced the series resistance of the solar cells, allowing the photovoltaic conversion efficiency of the solar cells to be increased. However, because they could outgrow on the silicon, a high number of extremely large Ag crystallites caused increased risk of etching the p-n junction. When the p-n junction was broken by oversized Ag crystallites, leakage current was generated in the solar cells, which would significantly reduce the shunt resistance and the photovoltaic conversion efficiency of the solar cells. Considering these opposing influences, to obtain solar cells with good electronic properties, the best proportion of Ag-Te alloy powder-doped glass frits was 5wt%.

References

1. M. Horteis, T. Gutberlet, A. Reller and S.W. Glunz, *Adv. Funct. Mater.*, 20 (2010) 476.
2. J.D. Fields, M.I. Ahmad, V.L. Pool, J. Yu, D.G.V. Campen, P.A. Parilla, M.F. Tony and M.F.A.M.V. Hest, *Nat. Commun.*, 7 (2016) 11143.
3. A.S. Ionkin, B.M. Fish, Z.R. Li, M. Lewittes, P.D. Soper, J.G. Pepin and A.F. Carroll, *ACS Appl. Mater. Interfaces.*, 3 (2011) 606.
4. Q. Che, H. Yang, L.Lu and Y. Wang, *J. Mater. Sci.: Mater. Election.*, 24 (2013) 524.
5. S.B. Cho, K.K. Hong, J.Y. Huh, H.J. Park and J.W. Jeong, *Curr. Appl. Apys.*, 10.2 (2010) S222.
6. M.I. Jeong, S.E. Park, D.H. Kim, J.S. Lee, Y.C. Park, K.S. Ahn and C.J. Choi, *J. Electrochem. Soc.*, 157.10 (2010) H934.
7. K.T. Butler, P.E. Vullum, A.M. Muggerud, E. Cabrera and J.H. Harding, *Phys. Rev. B: Condens. Matter*, 83.23 (2011) 2155.
8. J. Qin, W. Zhang, S. Bai and Z. Liu, *Sol. Energy Mater. & Sol. Cells*, 144 (2016) 256.
9. I. Karakaya and W.T. Thompson, *J. Phase Equilib.*, 12.1 (1991) 56.
10. K.K. Hong, S.B. Cho, J.S. You, J.W. Jeong, S.M. Bea and J.Y. Huh, *Sol. Energy Mater. & Sol. Cells*, 93 (2009) 898.
11. H. L. Lin, S. Y. Tsai, S. P. Hsu and M. H. Hsieh, *Sol. Energy Mater. & Sol. Cells*, 92 (2008) 1011.
12. J. Qin, W. Zhang, S. Bai and Z. Liu, M. M. Hilali, *Appl. Surf. Sci.*, 376 (2016) 52.
13. E. Cabrera, S. Oliber, J. Glatz-Reichenbach, R. Kopecek, D. Reinke and G. Schubert, *Energy Procedia*, 8.4 (2011) 540.
14. E. Cabrera, S. Oliber, J. Glatz-Reichenbach, R. Kopecek, D. Reinke and G. Schubert, *J. Appl. Phys.*, 110.11 (2011) 461.
15. D. Kim, S. Hwang and H. *Kim, J. Korean Phys. Soc.*, 55 (2009) 1046.
16. B.M. Boyerinas, J.M. Balsam, H.A. Baruck and A.L. Roytburb, *J. Appl. Phys.*, 113.18 (2013) 898.
17. O. Growski, L. Murawski and K. Trzebiatowski, *J. Phys. D. Appl. Phys.*, 15 (2000) 1097.
18. Y. Yang, S. Seyedmohammadi, U. Kumar, D. Gnizak, E. Graddy and A. Shaikh, *Energy Procedia*, 8 (2011) 607.